

The fabrication of a dip- coated tin oxide thin film via sol- gel processing and a study of its gas sensing properties

M. R.Vaezi* and M. Zameni

Division of Nanotechnology and Advanced Materials, Materials and Energy Research Center, MERC, Karaj, Iran

In this paper, tin oxide, SnO₂, thin films were coated on soda- lime glass substrates using the simple and economic processing route such as dip coating sol- gel method. In the preparation of a stable sol, instead of using only one alcohol, a combination of some alcohols without adding any surfactant and applying non- liquid tin chloride has been used. The effect of temperature, time, and thickness of the layers were studied. The phase and structural determination of samples were obtained by X-ray diffraction (XRD) analysis. Scanning electron microscopy (SEM) images were used for size and morphological evaluation of the thin films obtained. The gas- sensor response of tin dioxide thin films was determined by electrical sheet resistance measurements. After exposing the gas to different concentrations of ethanol, the effects of temperature, gas concentration, size, shape, dispersion of crystallite and thickness of the film on the sensor response were investigated. The best sensing responses are related to a two- times deposited layer with a thickness of about 299 nm heated at 400 °C and 600 °C. The first detection of gas concentration was at about 27.7 ppm ethanol at 300 °C. Also, the level of response and recovery times of this sensor were 70 and 88 s, respectively.

Key words: Sol-gel, Gas sensor, Tin oxide, Ethanol, Dip coating, Thin film.

Introduction

Among the various sensors which have been developed to detect gases, resistive sensors based on semiconductor oxides due to their low price, environmental compatibility, stability and tolerance to high temperature work, have a good potential for use in electronic detectors. Among them, tin oxide has been considered for its high sensor response to oxidizing and reducing gases simultaneously and its thermal stability. Tin oxide is an n-type semiconductor with a wide band gap of about 3.6 eV which has a tetragonal crystalline structure [1, 2].

The gas sensing mechanism of tin oxide thin films has long been studied, and the oxygen adsorption model [3], Schottky barrier model [4], the model controlled by gas penetration [1, 5] and the effect of grain size [6] are the objective explanations for the resistance reduction phenomenon of tin oxide against reducing gases. In this paper, the famous oxygen adsorption model has been considered to justify this phenomenon.

When tin oxide thin films are exposed to air, the physically adsorbed molecules take oxygen from the conduction band and are converted to the adsorbed O⁻ and O²⁻. These adsorbed molecules create an electron depletion layer just beneath the surface of tin oxide particles, and a potential barrier between particles is created; thus the tin oxide layer becomes highly

resistive. The reduction of the potential barrier occurs when the adsorbed oxygen is exposed to reducing gases, leading to an increase in the conduction of resistive film. Differences in the measured conductance against various gases depend on many parameters including the intrinsic resistance, grain size, grain boundaries, the inspection temperature, etc. [7].

Tin oxide layers have been prepared by different methods including sputtering [8], chemical vapor deposition (CVD) [9], pulsed laser deposition (PLD) [10] and different chemical routes such as spray pyrolysis [11], two stage chemical deposition (TSCD) [12], chemical bath deposition (CBD) [13] and sol gel processes [7, 14]. Within these methods, chemical methods such as CBD, TSCD and especially sol gel processes are useful methods because they are inexpensive and quite simple methods. Among all the chemical techniques, the sol gel process because of the ease of composition control, low processing temperature, large area coating, low equipment cost and good electrical and optical properties is particularly attractive [7, 14].

Ethanol vapor is one of the gases that are widely studied by metal oxide gas sensors; especially for leakage detection in industrial and distribution lines and in small medical devices to detect alcohol in exhaled human breath.

Experimental

Thin film fabrication

The gas sensing material, tin oxide (SnO₂), thin films

*Corresponding author:
Tel : +98-26-36280040
Fax: +98-26-36201888
E-mail: m_r_vaezi@merc.ac.ir

were prepared from a starting precursor via the sol-gel route. Pure SnO₂ sols were prepared from anhydrous SnCl₄, water, propanol (C₃H₇OH), and isopropanol (2-C₃H₇OH) at a molar ratio SnCl₄/H₂O/C₃H₇OH/2-C₃H₇OH = 1/9/9/6. At first, the SnCl₄ was dropped into two-thirds of the total amount of propanol. Then one-third of the total water dissolved in the remaining C₃H₇OH was added for prehydrolysis of the tin precursor. It was stirred for 1 h and after that the previously prepared sol was mixed with the solution of the remaining amount of H₂O dissolved in the prescribed amount of 2-C₃H₇OH. It was again stirred for 1 h. With this procedure, clear and homogeneous sols were prepared [7].

Thin films were deposited on soda-lime glass substrates using a dip-coating technique. Prior to the deposition, the substrates were cleaned first by washing liquid, followed by rinsing with de-ionized water and then in an ultrasonic device. The substrates again were washed by de-ionized water and dried with hot air. The cleaned glass substrates were then dipped into the sol and withdrawn at the rate of 6 cm·minute⁻¹ as shown in Fig. 1. Then they were clamped in a sealed container until the layers produced dried under their natural vapor pressure. To increase the rate of drying they could be set in an oven for half an hour at a temperature of about 50 °C. After these stages, the layers were heated in a furnace at 400 °C for half an hour and after cooling they were coated again, and this time they were heated at 600 °C for two hours. The conditions and the operating parameters of dip-coated films are shown in Table 1.

Characterization

For phase transformation evaluation at high temperature

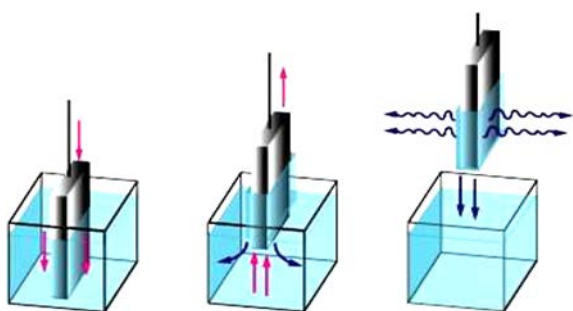


Fig. 1. Schematic diagram of the dip coating process used in this paper.

Table 1. The conditions and operating parameters of dip coated thin films.

| Name | No. of Deposited Layers | Sintering Temperature (First Layer) (°C) | Time of Treatment (First Layer) (h) | Sintering Temperature (Second Layer) (°C) | Time of Treatment (Second Layer) (h) |
|------|-------------------------|--|-------------------------------------|---|--------------------------------------|
| S1 | 2 | 400 | 0.5 | 600 | 2 |
| S2 | 2 | 400 | 0.5 | 500 | 1 |
| S3 | 1 | - | - | 600 | 2 |

an STA analyzer (STA 1640, Polymer Laboratories, England) was used.

SnO₂ thin films were characterized for their surface morphology, crystallite size, film thickness, phases present and preferred orientation. The microstructure of the layers was investigated by FE-SEM. The specimens were coated previously with a thin (around 20 nm) gold layer, which was sputtered on top of the samples to avoid charging effects. Specimens were observed at accelerating voltages (< 20 kV) using an Hitachi-S416 Japan field emission scanning electron microscope.

X-ray diffraction (XRD) was used to determine the phases present and the preferred orientation of the deposits. An Unisuntis XMD 300 X-ray diffractometer with Cu K α radiation ($\lambda = 1.5418$ Å) was employed to obtain XRD spectra using standard θ - 2θ geometry. A computer-base search and match was used for phase identification. Also, for determination of sintering temperature an STA analyzer was used.

Sensor fabrication and measurements

The films obtained sintered at 400 °C and 600 °C were considered as sensing elements. The metallization was carried out by paste printing of a high temperature conductive epoxy resin (Duralco-124). Two electrodes 2 mm \times 4 mm were deposited on each device. Thin Pt wires were cemented to the metallized area by the same epoxy. The sample was then gradually heated up to 200 °C to cure the epoxy and contact stabilization. The sample was then attached to a temperature-controlled micro-heater. A sensor probe was formed by mounting the sample on a borosilicate glass tubing, through which two insulated connection cables were guided to the temperature control unit and the impedance measurement device, respectively. The test gas was passed into the borosilicate glass tank.

The details of the construction and a schematic illustration of the fabricated gas sensor have been reported previously [15].

The ethanol sensing test was performed on the samples using the measurement of the sheet resistance of a SnO₂ thin film in air (R_a) and in the gases to be detected (R_g), and the results were recorded based on the temperature variations in a constant concentration and concentration changes at a constant temperature. For this test, the air of the chamber was contaminated with a certain level of target gas, and sensing rate or

the sensor resistance changes were calculated by the following equation:

$$R_s = (V_T/V_r - 1)R_r \quad (1)$$

where R_s is the sensor resistance, V_T is the voltage at the desired temperature, V_r is the voltage in the testing setup resistance, and R_r is the testing setup resistance. Also, the calculated sensor response value in the particular temperature or a concentration, $S_{T \text{ or } C}$, can be obtained from the following:

$$S_{T \text{ or } C} = \frac{R_a}{R_g} \quad (2)$$

where R_a is the sensor resistance in air, and R_g is the sensor resistance in the presence of gas [16].

Results and discussion

After preparing the desired sol according to the experimental section, the dried gel was prepared for DTA analysis to determine a drying and suitable sintering temperature. DTA analysis results for this sample are shown in Fig. 2. As it can be seen in Fig. 2, the appropriate temperatures for drying and sintering treatments are 50 °C and 400-600 °C, respectively.

Fig. 3 shows the X-ray diffraction pattern of a pure SnO₂ thin film compared to that of the reference (see {00-050-1429} in X'Pert software, Fig. 3a). All the

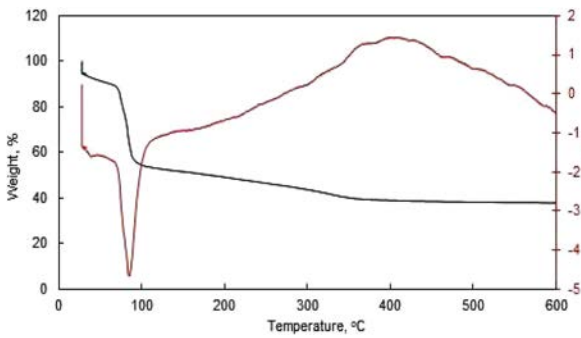


Fig. 2. DTA analysis result for the SnO₂ sol.

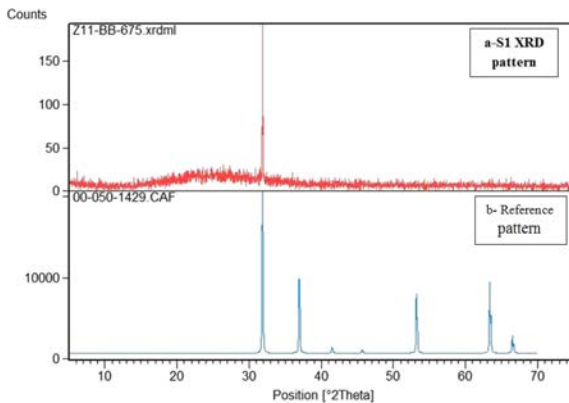


Fig. 3. XRD pattern of sample S1 (a) compared with the reference pattern (b).

spectra obtained showed typical tetragonal crystalline (Cassiterite) features.

Effect of temperature and concentration changes on the sensing behavior

Dynamic changes in the electrical resistance resulting from ethanol adsorption were measured on pure SnO₂ thin film. The experiments have shown that the operating temperature has a large influence on the gas sensor response. Fig. 4a shows the temperature dependence of the gas sensor response of a pure SnO₂ thin film at an ethanol concentration of 2500 ppm. Fig. 5 reports the ethanol sensor response versus its concentration at a constant temperature of 412 °C. The results reported were obtained from the data coming from the measurements carried out at the temperature where the maximum sensor response is reached. In all cases, the response of the analyzed thin films in a logarithmic plot (Fig. 4.b) is linear over a wide range of concentrations and, therefore, we conclude that the

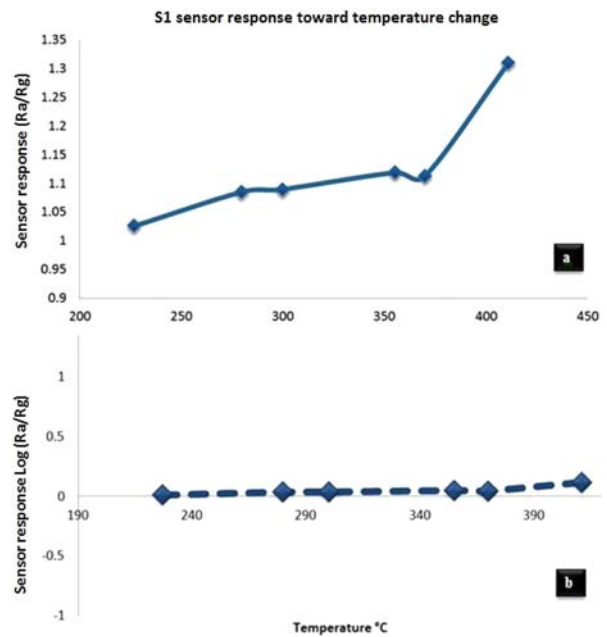


Fig. 4. The sensor response of a SnO₂ thin film to 2500 ppm ethanol as a function of temperature.

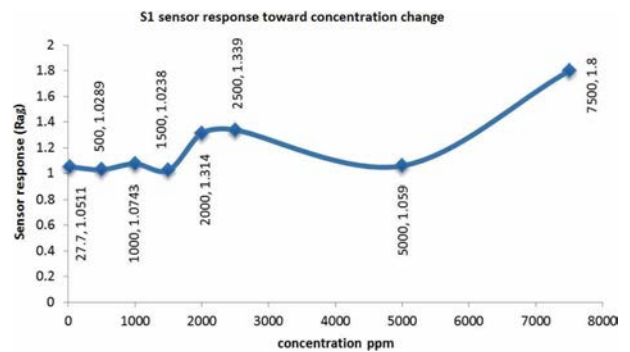


Fig. 5. The sensor response of a SnO₂ thin film to ethanol as a function of concentration at 412 °C.

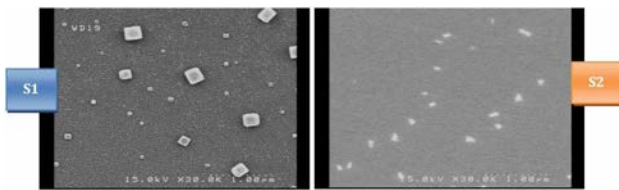


Fig. 6. FE- SEM images of samples S1 and S2.

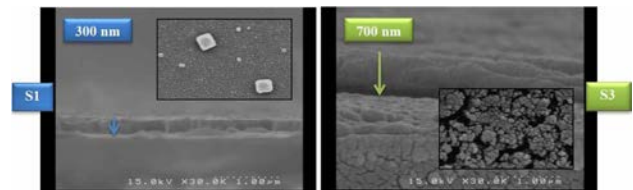


Fig. 8. The sectional FE- SEM images of samples S1 and S3.

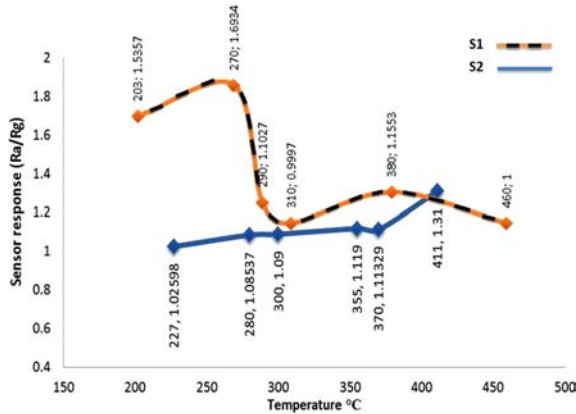


Fig. 7. The sensor response of samples S1 and S2 to 2500 ppm ethanol as a function of temperature.

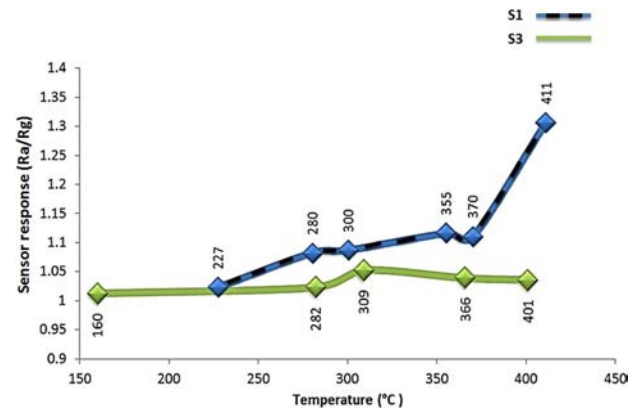


Fig. 9. The sensor response of e samples S1 and S3 to 2500 ppm ethanol as a function of temperature.

isothermal conductivities exhibit a power- low dependence.

As is shown in Figs. 4a and 5, the sample S1 indicates an acceptable sensing behavior over a wide range of concentrations and temperatures. Moreover, the level of the response and the recovery times for this sample are calculated as 70 and 88 s, respectively. In the next sections, the effect of two important factors on the sensing behavior are considered.

Effects of the crystallite shape and size on the sensing behavior

Fig. 6 shows FE- SEM images of samples S1 and S2. Fig. 7 shows the temperature dependence of the gas sensor response of the samples S1 and S2 at an ethanol concentration of 2500 ppm. From the evaluation of Figs. 6, 7; the effect of an inadequate sintering time and temperature on the sensing behavior can be understood. S1 distribution of crystallite size, was 20 nm, 100 nm and 220 nm, compared with numbers 300 nm, 20 nm for S2, plus their incomplete shape could be considered a good explain for the high undulation sensing changes.

Although S2 initially shows a higher degree of sensor response, the incomplete cube shape of tin oxide and natural lack of complete grain development has affected the surfaces that have the most important effects on the sensing behavior. Probably due to existence of very large grains along with very small ones, the first sensing is excellent, but because of very small grain diameter, the depletion layer become larger than the grains which prevents the reduction of the potential barrier, and also reduces the conduction and sensing values. Then, the initial grains are retrieved and

a sensing phenomenon was performed. As a result, enough growth time should be given to the film to become at least slightly larger than the depletion layer. This situation is achieved at the time and temperature for which sample S1 was prepared.

Effects of crystallite size distribution rate and thickness of layers on the sensing behavior

A look at the other two samples with a double and single layer that are shown in figures 8 and 9 establishes an interesting point. It was predicted that the thickness of layers and crystallite size in S1 is larger. But as can be seen in Fig. 8 the results were quite different.

The crystallite sizes of S3 are in the range of 35-100 nm and approximately 85% of them possess a crystallite size of 85 nm and in comparison with S1 had substantially grown. But in S1, 70% of grains are in the size range of 20-25 nm and 20% of them are in the size range of 220 nm. This phenomenon can justify this way that in the initial heating of sample S1 up to 400 °C, the grains grow to some extent and after the second coating and heating, the new grains grow to some extent, while the older ones have an opportunity to reach complete growth. The important point here is that the existence of coarse grains caused a restriction of grain boundaries, and prevented their excessive growth at high temperature and caused the thickness to be controlled; and also caused the removal of all half grown grains to help the growth of coarse ones. This phenomenon improves the sensor response level and trend in temperature. The appropriate crystallite size and controlling the layer thickness have

caused the dramatic differences in the ethanol gas sensing of these two samples. While the control of indiscriminate crystallite growth during heat treatment (which is a point of interest in the field of sensing) is achievable with this approach.

But the point that is noteworthy about thickness is that in the sensing behavior of sample S1, recorded much noise was recorded and a high swing in resistance and voltage, along with an excellent sensor response value that will give the desired sensing result. These problems are very rare in the thicker sensors. An optimum mode should therefore be considered as the depletion layer having enough space to exchange free oxygen.

Conclusion

Much effort has been spent to increase sensor response, decrease the response and recovery time and improve the selectivity of sensors. Part of this research has been dedicated to the impact of construction methods [8, 17-19], and the microstructure of sensitive layer [20-22] resulting in improved performance of sensors. For example, utilization of different dopants [14, 23] and molecular sieves [24], are two main methods to increase the response and the selectivity of these sensors. Solving the problems such as the control of grain size during heat treatment, the working temperature, the thermal and mechanical stability, the porosity distribution value [25, 26] and the stability are considered to be most research goals in the process of making a sensor.

That is why in this study, tin oxide was selected as one of the best metal oxide resistant sensors in response to various gases, with a sol based on multiple alcohol and dried tin chloride as the best precursor to producing a homogeneous, stable and good adhesive thin film. Also with use of dip coating as a cheap, simple and suitable method to coat all simple and complex shapes. We then attempted to adjust the number of coating layers and speed of coating, set the size and shape of crystallites with a control of the temperature and sintering time, to achieve a cheaper and easier gas sensor, while showing a remarkable amount of sensor response, response and recovery time and stability. Also, by reducing the thickness to the nano-meteric limit an attempt was made to prevent grain growth in the operating temperature or sintering temperature.

References

1. Shuping Gong, Jianqiao Liu, Jing Xia, Lin Quan, Huan Liu and Dongxiang Zhou, *Materials Science and Engineering B* 164 (2009) 85-90.
2. Th Diana, K. Nomita Devi and H. Nandakumar Sarma, *Indian Journal of Physics* 84 (2010) 687-691.
3. C. O. Par and S. A. Akbar, *Journal of materials Science* 38 (2003) 4611-4637.
4. S. Roy Morrison, *Sens. Actuators B* 11 (1987) 283-287.
5. G. Sakai, N. Matsunaga, K. Shimano and N. Yamazoe, *Sens. Actuators B* 80 (2001) 125-131.
6. C. Xu, J. Tamaki, N. Miura and N. Yamazoe, *Sens. Actuators B* 3 (1991) 147-155.
7. Sunita Mishra, C. Ghanshyam, Nathai Ram, Satinder Singh, R. P. Bajpai and R K Bedi, *Bull. Mater. Sci.* 25 (2002) 231-234.
8. D. Haridas, K. Sreenivas and V. Gupta, *Sensors and Actuators B* 133 (2008) 270-275.
9. A.A. Hosseini and F. Taleshi, *Indian Journal of Physics* 84 (2010) 789-794.
10. S. Gupta, R. K. Roy, M. Pal Chowdhury and A. K. Pal, *Vacuum* 75 (2004) 111-119.
11. Arturo I. Martinez, Dwight R. Acosta, *Thin Solid Films* 483 (2005) 107-113.
12. S.K. Sadmezhad, M.R. Vaezi: *Ceram. Inter.* 33 (2007) 1409-1417.
13. Y. Lare, A. Godoy, L. Cattin, K. Jondo, T. Abachi, F.R. Diaz, M. Morsli, K. Napo, M.A. del Valle, J.C. Bernède, *Appl. Surf. Sci.* 255 (2009) 6615-6619.
14. Viviany Geraldo, Luis Vicente de Andrade Scalvib, Evandro Augusto de Moraisa, Celso Valentim Santillic and Sandra Helena Pulcinellc, *Materials Research* 6 (2003) 451-456.
15. M.R. Vaezi, *Mater. Chem. Phys.* 110 (2008) 89-94.
16. Jianqiao Liu, Shuping Gong, Jing Xia, Lin Quan, Huan Liu and Dongxiang Zhou, *Sensors and Actuators B* 138 (2009) 289-295.
17. Ki-Won Kim, Pyeong-Seok Cho, Sun-Jung Kim, Jong-Heun Lee, Chong-Yun Kang, Jin-Sang Kimb and Seok-Jin Yoon, *Sensors and Actuators B* 123 (2007) 318-324.
18. Bogusława Adamowicz, Weronika Izydorczyk, Jacek Izydorczyk, Andrzej Klimasek, Wiesław Jakubik and Janusz Źywicki, *Vacuum* 82 (2008) 966-970.
19. Gong Shuping, Xia Jing, Liu Jianqiao and Zhou Dongxiang, *Sensors and Actuators B* 134 (2008) 57-61.
20. Jin-Ah Park, Jaehyun Moon, Su-Jae Lee, Seong Hyun Kim, Hye Yong Chu and Taehyoung Zyung, *Sensors and Actuators B* 145 (2010) 592-595.
21. Xiaofeng Song, Dejiang Zhang and Meng Fan, *Applied Surface Science* 255 (2009) 7343-7347.
22. J. Kaur, V.D. Vankar, M.C. Bhatnagar, *Sensors and Actuators B* 133 (2008) 650-655.
23. W. Liu and L.Cao, *Science in China Series B: Chemistry* 44 (2001) 63-67.
24. A. Keshavaraja, B.S. Jayashri, A.V. Ramaswamy and K. Vijayamohan, *Sensors and Actuators B* 23 (1995) 75-81.
25. C. Goebbert, R. Nonninger, M.A. Aegerter and H. Schmidt, *Thin Solid Films* 351 (1999) 79-84.
26. Faramarz Hossein-Babaei, Mohammad Orvatinia, *Sensors and Actuators B* 89 (2003) 256-261.